Fuel 96 (2012) 374–382

Contents lists available at SciVerse ScienceDirect

Fuel

journal homepage: www.elsevier.com/locate/fuel

Experimental investigation of a biomass-fired ORC-based micro-CHP for domestic applications

Guoquan Qiu, Yingjuan Shao, Jinxing Li, Hao Liu *, Saffa .B. Riffat

Department of Architecture and Built Environment, Faculty of Engineering, University of Nottingham, University Park, Nottingham NG2 2RD, UK

ARTICLE INFO

Article history:
Received 14 August 2011
Received in revised form 15 January 2012
Accepted 16 January 2012
Available online 27 January 2012

Keywords:
Micro-CHP
Organic Rankine cycle (ORC)
Vane expander
HFE7000
Biomass-fired

ABSTRACT

The ever-increasing global energy demand and the mounting environmental concerns caused by the increasing consumption of fossil fuels call for more and more utilisation of sustainable energy sources such as biomass. Many medium- and large-scale biomass-fired combined heat and power (CHP) plants have been demonstrated and commercialised in many parts of the world, such as several European countries and China. However, few biomass-fuelled micro-scale CHP (1–10 kW_e) systems suitable for domestic applications have been demonstrated or commercialised. This paper presents the preliminary results of an experimental investigation on the biomass-fired organic Rankine cycle (ORC)-based micro-CHP system currently developed by the authors. The biomass-fired ORC-based micro-CHP system mainly consists of a biomass boiler, an evaporator, an ORC expander, an alternator, a heat recuperator and a condenser. The heat of biomass combustion in the boiler is used to generate hot water, which is then used to heat and vaporise the organic working fluid through the evaporator. The organic fluid vapour drives the expander to rotate an alternator, producing power. The expanded organic fluid vapour leaving the expander first passes through the heat recuperator and then is condensed in the condenser. The cooling water leaving the condenser can be heated to a temperature (~46 °C) suitable for domestic washing and underfloor heating etc. Testing results of the micro-CHP system with a 50 kW_{th} biomass-pellet boiler are analysed and presented in this paper. The current micro-CHP generated 861 W electricity and 47.26 kW_{th} heat, corresponding to electricity generation efficiency of 1.41% and CHP efficiency of 78.69%. Further improvements on the performance of the expander and the alternator assembly as well as the design of the biomass boiler's heat exchanger need to be addressed in the future.

1. Introduction

The continual uses of fossil fuels to meet our ever-increasing energy demands have led to environmental pollution to air, water and land. Renewable energy sources are alternatives to the depleting fossil fuels and offer improved security of our future energy supply. Biomass energy, a traditional renewable energy source, currently ranks fourth worldwide providing approximately 14% of the world's primary energy supply. In developing countries, biomass accounts for approximately 35% or higher of the primary energy supply [1]. Combustion is the most widely used technology to convert bulky, solid biomass feedstock into useful forms of energy due to its simplicity and maturity. Although biomass combustion releases carbon dioxide (CO_2), similar to the combustion of fossil fuels, it is a CO_2 neutral process as the same amount of CO_2 in the atmosphere was absorbed by the growing biomass plants via photosynthesis a short time (ca. a year to 10 years) ago. In addition, the emissions of SO_x and NO_x from the combustion of many biomass fuels are insignificant, particularly compared to coal combustion. The ever-increasing global energy demand, depleting fossil fuel reserves and global warming require a further increase in biomass energy utilisation for distributed electricity generation and domestic heating in both developing and developed countries. Biomass-fuelled CHP systems can efficiently convert biomass chemical energy into electricity and heat. Biomass energy has its advantage of continuity over the intermittence of solar energy and wind energy. In considering the merits of biomass energy, biomass-fuelled CHP systems have the potential to solve the energy trilemma, i.e., security of supply, affordability of energy and environmental protection [2].

Biomass CHP systems have received a great deal of attention over the past decade [3–5]. Large and medium-scale CHP plant technologies based on biomass combustion have now reached a high level of maturity. Biomass CHP plants larger than 2000 kW_e, mostly based on biomass combustion and using steam turbines to produce electricity, have been in commercial applications for over a decade [4,5]. However, high temperature and high pressure steam as the working fluid of a steam Rankine Cycle turbine for a smaller CHP system would result in not only an expensive complex

* Corresponding author. Tel.: +44 115 8467674; fax: +44 115 9513159.
E-mail address: liu.hao@nottingham.ac.uk (H. Liu).

0016-2361
doi:10.1016/j.fuel.2012.01.028

Nomenclature

CV	calorific value of biomass fuel (Wh/kg)
h	organic working fluid enthalpy (kJ/kg K)
h_{evap_in}	water enthalpy at the inlet of evaporator (kJ/kg)
h_{evap_out}	water enthalpy at the outlet of the evaporator (kJ/kg)
h_{cond_in}	water enthalpy at the inlet of condenser (kJ/kg)
h_{cond_out}	water enthalpy at the outlet of the condenser (kJ/kg)
$\dot{m}$	organic working fluid mass flow rate (kg/s)
$\dot{M}_{burn}$	biomass consumption rate (kg/h)
$\dot{m}_{h\_w}$	hot water flow rate (kg/s)
$\dot{m}_{c\_w}$	cooling water flow rate (kg/s)
P_{ex_in}	pressure at expander inlet (bar)
P_{ex_out}	pressure at expander outlet (bar)
Q_{burn}	thermal input to the biomass boiler (kW)
Q_{c_w}	heat absorbed by cooling water in the condenser (kW)
Q_{in}	heat entering ORC from boiler (kW)
W_{ele}	electric power output (kW)
W_{net}	net work of ORC (kW)
W_p	work of the pump (kW)
W_{ex}	ideal work output of the expander (kW)
W_{ex_act}	actual work output of the expander (kW)

Greek letters

η_{boiler}	biomass boiler efficiency
η_{CHP}	total CHP efficiency
η_{ele}	electrical efficiency
η_g	generator (alternator) efficiency
η_{ORC}	thermal efficiency of ORC
η_{ex}	expander efficiency
η_{th}	thermal efficiency

system but also safety concerns for some users. In the medium-scale power range (200–2000 kW_e) and small-scale range (<200 kW_e), a suitable organic fluid, instead of water/steam, can be used as the working fluid of a Rankine cycle turbine due to its technological suitability and economic sustainability. CHP systems with organic Rankine cycle (ORC) operate at lower pressures and temperatures than CHP systems with steam turbines, reducing system cost and complexity and alleviating safety concerns. The medium-scale biomass-fired ORC-based CHP plants have already been successfully demonstrated in Admont (400 kW_e) and Lienz (1000 kW_e) [1,4], which use silicon oil as working medium and thermo-oil as heating medium, achieving ca.18% electrical efficiency and 80% overall CHP efficiency. Although ORC-based power generation has been widely applied to the power generation from low temperature heat sources, such as the recovery of industrial waste heat, geothermal heat and solar heat with a size as small as a fraction of 1 kW_e [6], few have investigated the development of micro-scale biomass-fired ORC-based CHP units (<10 kW_e) which have a great potential to meet the energy needs of residential buildings. The authors are currently developing and evaluating a 1 kW_e micro-scale biomass-fired ORC-based CHP system in the University of Nottingham [1]. This paper presents the latest results of the on-going laboratory testing of the micro-CHP system.

2. The proposed biomass-fired micro-CHP with ORC

2.1. Organic Rankine cycle for biomass-fired micro-CHP system

On many occasions, organic Rankine cycle engines were rejected with CHP systems because of their relatively low electrical conversion efficiency. However, as electrical efficiency comes to be considered a less important issue for micro-CHP, organic Rankine cycle engines are again phased in due to their relative simplicity (low costs), favourable durability and performance characteristics. Fig. 1 shows the ORC layout and T–S chart of the proposed biomass-fired micro-CHP system. The proposed micro-CHP system mainly consists of two cycles: the hot water cycle heated by a biomass boiler and the organic Rankine cycle. The heat released from the combustion of biomass inside the biomass boiler is used to heat the water through the boiler heat exchangers, whereas the hot water is used to heat the ORC working fluid into vapour in the evaporator. The generated organic vapour drives the expander to rotate an electric generator, producing power. The working fluid at the expander exhaust releases some heat through the recuperator to heat the condensed ORC fluid and then is condensed in the condenser and pumped back to the evaporator, beginning a new cycle. The cooling water leaving the condenser is heated and can be used for domestic washing, hot water supply or under-floor heating etc. The total CHP efficiency of the proposed micro-CHP system has been predicted to be able to reach 80% or higher and the electrical efficiency to 10% or higher [7,8]. The modelling also showed that the electric efficiency of the micro-CHP system could be increased by using internal heat recuperation [7], minimising superheating of the ORC vapour at the expander inlet and minimising subcooling of the ORC liquid at the condenser outlet [7,8]. As can be seen from Fig. 1, the Rankine cycle is a closed loop cycle. Therefore, mass conservation of working fluid and the first law of thermodynamics can be applied to the analyses of the ORC at steady state. The ideal work output of the expander W_{ex} and work of the pump W_p can be expressed as:

$$W_{ex} = \dot{m}(h_4 - h_5) \tag{1}$$

$$W_p = \dot{m}(h_2 - h_1) \tag{2}$$

where $\dot{m}$ is the working fluid mass flow rate (kg/s).

The net work of the ORC can be expressed as:

$$W_{net} = W_{ex} - W_p = \dot{m}[(h_4 - h_5) - (h_2 - h_1)] \tag{3}$$

The heat transfer supplied by the biomass boiler via the evaporator is:

$$Q_{in} = \dot{m}(h_4 - h_3) \tag{4}$$

The thermal efficiency of the ORC can be expressed as the net work of the ORC divided by the heat input into the ORC:

$$\eta_{ORC} = \frac{W_{net}}{Q_{in}} \tag{5}$$

The expander efficiency is the ratio between the actual work output and the ideal work output and can be expressed as:

$$\eta_{ex} = \frac{W_{ex\_act}}{W_{ex}} = \frac{h_4 - h_{5'}}{h_4 - h_5} \tag{6}$$

The generator (alternator) efficiency η_g can be expressed as the power output W_{ele} divided by the actual work output from the expander (i.e. shaft power),

$$\eta_g = \frac{W_{ele}}{W_{ex\_act}} = \frac{W_{ele}}{\dot{m}(h_4 - h_{5'})} \tag{7}$$

where W_{ele} is evaluated by the electric load.

For the hot water loop, the biomass boiler efficiency can be defined as the ratio between the heat released by the hot water through the evaporator and the thermal input to the boiler,

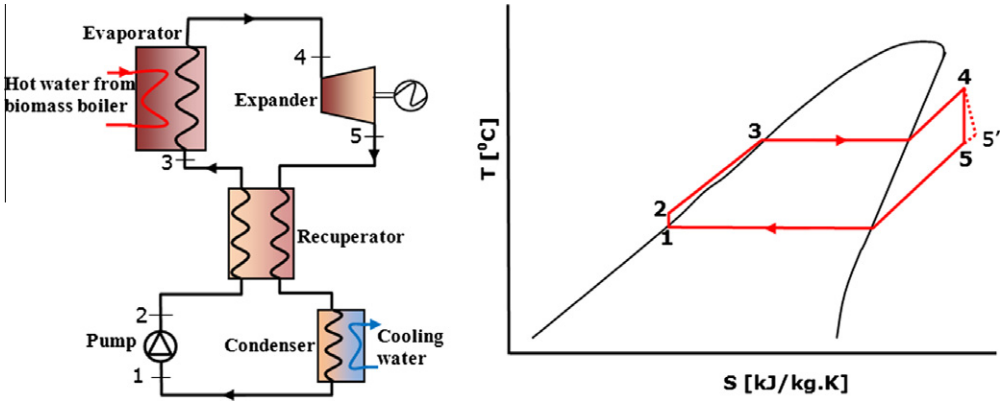

Fig. 1. Biomass-fired CHP: organic Rankine cycle layout and T–S chart.

$$\eta_{boiler} = \frac{Q_{h\_w}}{Q_{burn}} = \frac{\dot{m}_{h\_w}(h_{evap\_in} - h_{evap\_out})}{Q_{burn}} \quad (8)$$

where $\dot{D}_{h\_w}$ is hot water flow rate; h_{evap_in} and h_{evap_out} are hot water enthalpies at the inlet and outlet of the evaporator, respectively. Q_{burn} can be calculated with the biomass consumption rate $\dot{M}_{burn}$ and the calorific value (CV) of the biomass fuel:

$$Q_{burn} = \dot{M}_{burn} \times \mathrm{CV} \quad (9)$$

The boiler efficiency is to be evaluated on low heating value (LHV) and hence CV in the above equation is replaced by LHV.

The heat absorbed by the cooling water in the condenser is:

$$Q_{c\_w} = \dot{m}_{c\_w}(h_{cond\_out} - h_{cond\_in}) \quad (10)$$

where $\dot{m}_{c\_w}$ is cooling water flow rate; h_{cond_out} and h_{cond_in} are cooling water enthalpies at the outlet and inlet of the condenser, respectively.Therefore, the electrical efficiency η_{ele}, thermal efficiency η_{th} and total CHP efficiency η_{CHP} can be assessed as [9]:

$$\eta_{ele} = \frac{W_{ele}}{Q_{burn}} \quad (11)$$

$$\eta_{th} = \frac{Q_{c\_w}}{Q_{burn}} \quad (12)$$

$$\eta_{CHP} = \eta_{ele} + \eta_{th} = \frac{W_{ele} + Q_{c\_w}}{Q_{burn}} \quad (13)$$

2.2. Selection of expander and organic working fluid for the organic Rankine cycle

In order to improve the cycle efficiency, the selections of the expander and working fluid are of considerable importance to the biomass-fired ORC-based micro-CHP system. Recently, Qiu et al. [2] reviewed the state-of-the-art of micro-scale ORC expanders and concluded that scroll expanders and vane expanders were likely to be the good choices for 1–10 kW_e micro-CHP systems. Lemort et al. [10] and Quoilin et al. [11] investigated a scroll expander integrated into an organic Rankine cycle. Peterson et al. [12,13] studied a micro-scale scroll expander using different refrigerants (R123 and R134a) to achieve different testing results. Pei et al. [14] investigated the performance of a made-in-house radial-axial expander integrated into an organic Rankine cycle. Recently vane expanders for micro-CHP systems have received great interests and have been applied to transcritical CO_2 refrigeration cycles [15–23]. Peng and Yang et al. [15–17] and Jia et al. [18] investigated their made-in-house vane expanders experimentally and theoretically. Liu et al. [19] simulated a semi-hermetic scroll expander-generator with the ORC to convert the thermal energy from high-pressure vapour into electricity directly. A revolving piston-vane expander was used in the transcritical CO_2 refrigeration cycle by Subiantoro and Tiow [20], Subiantoro and Ooi [21] and Li et al. [22]. Wang et al. [23] used the made-in-house revolving piston-vane expander and working fluid R245fa in an organic Rankine cycle to achieve an average shaft power output of 1.64 kW and an average isentropic efficiency of 45.2% driven by the low-temperature solar thermal energy at a low working pressure.

Currently a micro-scale expander for organic working fluids is not commercially available and therefore a replacement of expander, modified from an air motor, is used in the present experimental setup [2]. The air motor, also called compressed-air-driven vane-type air expander, is of the volume type. The air motor-modified expander works on the reverse working principle of a vane-type compressor, as shown in Fig. 2. Expansion takes place when the chamber spaces between the sliding vanes in a rotor increase as the rotor turns clockwise within an eccentric cylinder (housing). The rotor has 4 longitudinal slots in which the vanes slide freely and move outward by centrifugal force against the cylinder wall of the stator. The highly compressed organic working fluid vapour rushes into the inlet port to form a chamber (A) and rotates the rotor. The trapped vapour is expanded as the volume of the chamber increases until the leading vane of the chamber passes the outlet port. The vapour volume expansion results in the pressure differences among the chambers, which drive the rotor turning.

For a safe and efficient system, the selection of working fluids is another important issue to achieve energy-efficient ORC. Compared with conventional water steam cycles, an organic fluid with lower working pressure and temperature means better safety for domestic applications. Three different types of slope in the saturation vapour curves of T–S diagrams may categorise organic fluids into three groups [24]: dry fluids which have positive slope and generally of high molecular mass; isentropic fluids which have nearly vertical saturation vapour curves and commonly of medium molecular mass; wet fluids which have negative slope and are of low molecular mass. The dry or isentropic fluids in the expander are generally vapour or superheating vapour without the danger of damaging the expander, but wet fluids with the condensate droplets in the expander, such as water, are inappropriate for ORC.

Working fluid selection for ORC has been investigated by many researchers [25–30]. Generally, the criteria to select a suitable working fluid are mainly based on the ORC application (e.g. the heating source characteristics) and the fluid's properties such as boiling temperature, expansion in superheating state, heat of vaporisation, heat transfer characteristics, toxicity, ozone depletion, thermal stability and flammability, as well as the fluid's cost. Several possible organic working fluids for various ORC

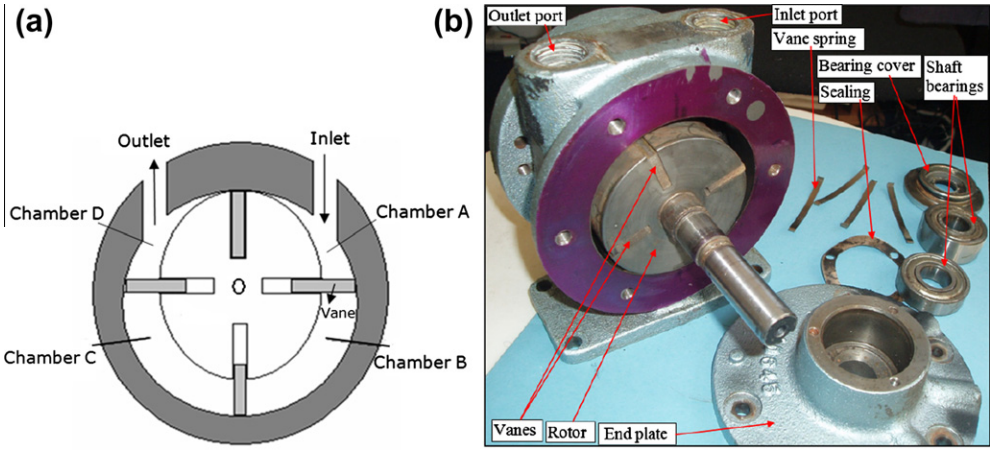

Fig. 2. Vane-type air motor as an expander [2].

Table 1
Main thermodynamic properties of organic fluids and water (in order of decreasing boiling points).

Fluid name	Molecular formula	M (g/mol)	T_{bp} (°C)	T_{crit} (°C)	P_{crit} (MPa)	Vaporisation heat H_{fg} at 1 bar (kJ/kg)	Saturation dome shape
Water	H_2O	18	100	373.95	22.06	2257	Wet
HFE71000	$CH_3OC_4F_9$	250	61	195.3	2.23	112	Dry
R-601 (*n*-pentane)	$CH_3(CH_2)_3CH_3$	72	35.5	196	3.36	358.7	Dry
HFE7000	$CH_3OC_3F_7$	200	34	165	2.48	142	Dry
R123	$C_2HCl_2F_3$	152.9	27.8	183.7	3.66	170.3	Dry
R245fa	$CF_3CH_2CHF_2$	134	15	154	3.64	196.9	Isentropic

applications are characterised and compared with water in Table 1. Mago et al. [31] investigated the effect of the fluid boiling point temperature on the performance of ORCs. The working fluids under investigation included R134a, R113, R245ca, R245fa, R123, isobutene and propane, with boiling points between −42.09 and 47.59 °C. They found the fluid that showed the best thermal efficiency was the one that has the highest boiling point among the selected fluids (R113, boiling point 47.59 °C), whereas the fluid that showed the worst thermal efficiency has the lowest boiling point temperature (propane, boiling point −42.09 °C). They concluded that the higher the boiling point temperature of the organic fluid the better the thermal efficiency that can be achieved by the ORC. It should be noted that R113 has a very high ozone depleting potential (ODP) and was phased out in 1996 by the Montreal protocol. As a consequence of phasing out R113, R123 has been widely applied in the ORC-based micro-CHP systems [10–12,14]. However, R123 also has the problem of a non-null ODP and will be phased out at the latest in 2030 depending on national legislations. HFE7000 may replace R123 in some applications due to its zero ODP [32].

As HFE7000 and HFE7100 have zero ODPs, appropriate boiling points at 34 °C and 61 °C, heat of vaporisation at 142 kJ/kg and 112 kJ/kg, respectively, and other favourable thermodynamic properties, they have been selected and tested by the authors as the working fluids of the micro-CHP system under investigation.

3. Experimental setup

So far, the testing of the micro-CHP system has been conducted with three different hot water boilers: a 9 kW electric boiler, a 25 kW_{th} biomass boiler [1] and a 50 kW_{th} biomass boiler, respectively. The electric boiler can provide the ORC with the stable heat output but it can only provide a maximum heat output of 9 kW, with the maximum temperature of the hot water being at 115 °C. The maximum electric power generated by the micro-CHP driven by the electric boiler was only 96 W [1]. The 25 kW_{th} biomass boiler, which is able to supply hot water at the maximum temperature of 115 °C, was used to replace the electric boiler and this led to better electric power output at 284 W [1]. After further improvement with individual components of the micro-CHP system such as bigger heat exchangers for evaporator and recuperator and better pipe connections between the expander and the heat exchangers, the micro-CHP system has been further tested with a 50 kW_{th} biomass boiler which was designed with the aim to provide hot water at the maximum temperature of 180 °C. Although two organic working fluids (HFE7100 and HFE7000) were initially tested with the biomass boilers, the power output was always somewhat higher (ca. 10% more power output) when HFE7000 was used as the working fluid under otherwise identical experimental conditions. As one of the main aims of the research was to maximise the power output of the micro-CHP system, HFE7000 was chosen as the main ORC working fluid with the 50 kW_{th} biomass boiler tests. This paper presents the latest experimental results of the micro-CHP system tested with the 50 kW_{th} biomass boiler.

3.1. The experimental micro-CHP system

The experimental micro-CHP system consists of three loops: the closed hot water loop, the closed organic Rankine cycle loop and the open cooling water loop, as shown in Fig. 3, where temperatures and pressures are labelled at main points in a typical CHP test. The hot water transfers heat from the biomass boiler into the ORC through the evaporator and the superheater – the two compact brazed plate heat exchangers. Hot water pump is mounted at the inlet of the biomass boiler since it is only able to withstand maximum operating temperature of 110 °C. A recuperator, a reservoir, a sight glass and a receiver vessel with vacuum pump are applied in the organic Rankine cycle loop. As predicted by thermodynamic modelling [7], the recuperator can improve

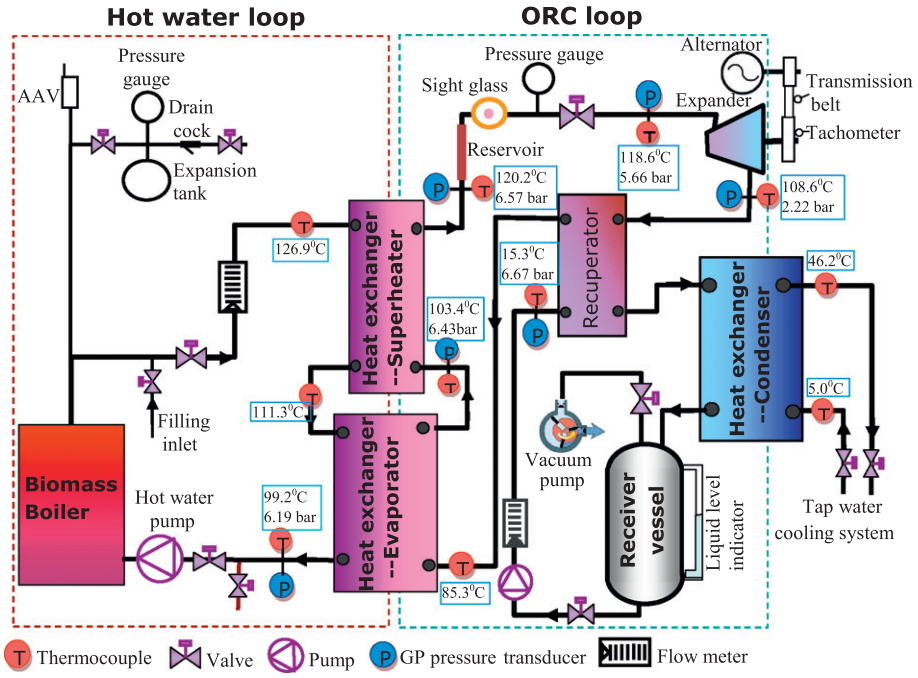

Fig. 3. Schematic of biomass-fired micro-scale CHP system with ORC.

Fig. 4. 50 kW_{th} wood pellet boiler and its combustion chamber and flame.

the ORC efficiency. The vertical section of the 28 mm in diameter pipe is used as the reservoir of the organic working fluid vapour. The reservoir can stabilize the pressure of the organic working fluid vapour and return the possible condensate of the organic working fluid back to the superheater along its inner wall. The quality of the organic working fluid vapour can be observed via the sight glass to ensure only vapour entering the expander. The receiver vessel can store the organic liquid where liquid level can be observed by the transparent liquid level indicator. Before starting the boiler to heat the CHP system, the vacuum pump can be used to vacuum the ORC loop. Replacing the vacuum pump with a bottle of organic working fluid, the evacuated receiver vessel can suck in the organic fluid and this is used as a means to top up the working fluid amount in the ORC loop. Fig. 4 shows the 50 kW_{th} wood pellet boiler used in the present experimental CHP system. The wood pellets are transported automatically by a screw auger conveyor from the hopper to the furnace. The biomass combustion is controlled with the primary air supply from the holes on the wall of the combustion bed and the second air supply from the four pipe jets around the flame. The mains water is used to cool the organic vapour

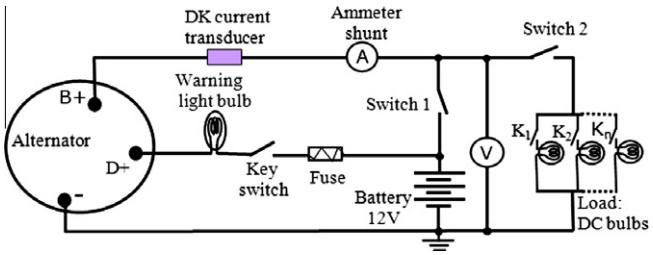

Fig. 5. Electric output circuit for the micro-CHP system.

Table 2
Excitation and power output of the alternator (Bosch alternator 140 A, 14 V).

Switch name	Switch 1	Switch 2	Key switch	Switch K_1, K_2,...,K_n
Alternator excitation	On	Off	On	Off
Battery charging	On	Off	Off	Off
Load output	Off	On	Off	On
Batter charging & load output	On	On	Off	On

through the condenser and the resulting warm water's temperature is continuously measured during testing.

An automotive alternator (Bosch alternator 140 A, 14 V) is driven by the expander to generate DC current and voltage. To measure the power output and to excite the alternator, an appropriate alternator circuit has been set up as shown in Fig. 5. A DK current transducer and voltmeter are connected to the data-taker DT80 so that transient currents and voltages are recorded by a computer. A mechanical ammeter and voltmeter are also used to indicate the current and voltage. In order to excite the alternator, Switch 1 (Fig. 5) is kept on at first and then the Key Switch (Fig. 5) is switched on. While the alternator produces magnetic field, the expander rotation speed decreases sharply. Other cases for the states of the electric switches are listed in Table 2. With the load output state, i.e. with the load – DC bulbs being added, the total current output may increase but the voltage may decrease. An optimal match of the current and the voltage can lead to the maximum electric output as the electric output is the product of the current and the voltage.

3.2. Experimental procedures

Before the biomass boiler is ignited, the hot water loop is filled up with mains water. The amount of organic working fluid in the ORC loop is adjusted to ensure that the liquid level in the receiver vessel reaches the pre-determined minimum level – if there is not enough organic working fluid in the ORC loop and the receiver vessel, the organic working fluid pump will not be able to keep the fluid continuously cycling within the loop. After the boiler is started, the hot water temperature rises up gradually. As soon as the set temperature of the hot water of the boiler is reached, the ORC performance testing (with no excitation of the alternator and hence without power generation) of the CHP system can be started by switching on the organic working fluid pump with a given load setting. The pump load setting may be changed from 1% to 100% of its capacity by an electric controller. The rotation speed of the expander will increase with increasing the pump load setting until there is organic working fluid moisture appearing at the inlet of the expander when the ORC performance testing is usually stopped. With the current experimental CHP system, the organic working fluid moisture would not appear at the inlet of the expander if the hot water flow rate is kept at 28.27 l/m and the hot water temperature is at 127 °C or above, even at the pump load of 100%. After the ORC performance testing, electricity generation testing of the CHP system can be carried out with the alternator being excited and the organic working fluid pump being set at 100% or another appropriate level of its capacity. Different electric loads can lead to various electric power outputs with a fixed organic working fluid pump load setting.

4. Results and discussion

4.1. ORC performance test without power generation

Before the alternator is excited, the ORC performance may be examined in the different refrigerant pump capacity. The main aims to carry out the ORC performance testing are to quickly examine the variations of the parameters (e.g. RPM of the expander, the pressure at the expander inlet, the pressure drop over the expander and the refrigerant flow rate) with increasing refrigerant pump capacity, as shown in Table 3 and Fig. 6, and to compare the parameter variations with and without power generation at the same refrigerant pump capacity. For instance, the refrigerant pump capacity was set at 65%, 70%, 75%, 85%, 90%, 95% and 100%, all the parameters, such as temperatures, pressures, the organic working fluid flow rate, would accordingly vary, as shown in Table 3. Although the biomass boiler was designed with the aim to supply hot water with the maximum temperature of up to 180 °C, it has been unable to generate hot water at a temperature of anywhere near 180 °C with any of the 3 hot water pump flow settings. When the maximum hot water temperature was set at 145 °C with the boiler control panel, the actual maximum boiler outlet water temperature that could be achieved was 128.9 °C (Table 3) with the present settings of the CHP system. As the actual hot water temperature could not reach the setting point of 145 °C, the boiler would not stop or reduce its load but instead continuously operated at its designed load, providing a stable heat to the organic Rankine cycle which can be considered as somewhat beneficial for the evaluation of the micro-CHP system. If the boiler hot water temperature is set at a lower point, for example, 120 °C, the boiler will reduce its load and stop operation for a while after reaching its set point of the hot water temperature and re-start operation after the hot water temperature drops by 2 °C below the set point. During the interval between the stop and the restart, termed as 'idle period', the boiler can emit a significant amount of carbon monoxide as quantitatively proved by the measurements with the 25 kW_{th} biomass boiler [33]. Therefore, the operation of the biomass-fired micro-CHP should be closely matched with the load demands of its user so that the idle period can be minimised, consequently minimising CO emissions. Although the hot water temperature could not rise to the set point of 145 °C, the organic working fluid flow rate, RPM of the expander and the pressure of the ORC increase with increasing the refrigerant pump capacity, as shown in Fig. 6. At the organic working fluid pump capacity of 100%, the organic working fluid states may be illustrated by the T–S chart as shown in Fig. 7. The thermodynamic properties of the organic working fluid – HFE7000 in Fig. 7 were predicted by use of the EES software [34]. EES stands for Engineering Equation Solver and is a general equation-solving program that can numerically solve thousands of coupled non-linear algebraic equations [34]. A major feature of EES is the high accuracy thermodynamic and transport property database that is provided for hundreds of substances (including HFE7000 and HFE7100) in a manner that allows it to be used with the equation solving capability of the Software [34]. The shape of the working T–S chart differs from the ideal one in Fig. 1 as the real working system has some irreversible losses (such as pressure losses).

Table 3
Typical variations of flow rate, temperature & pressure in ORC under various pump capacities of an ORC performance test (without power generation).

ORC pump capacity (%)	65	70	75	85	90	95	100
Expander RPM	1215	1228	1326	1588	1655	1677	1700
Alternator RPM[a]	2408	2434	2628	3147	3280	3324	3369
HFE7000 flow rate $\dot{m}$ (kg/min)	12.54	13.65	14.59	16.34	17.50	18.44	19.18
Boiler inlet water T (°C)	95.9	99.8	101.8	101.3	100.3	98.7	96.6
Boiler outlet water T °C	117.8	123.0	126.5	128.9	128.8	128.0	126.6
Expander inlet HFE7000 T (°C)	116.2	121.3	124.6	126.6	126.3	125.3	123.2
Expander outlet HFE7000 T (°C)	109.8	116.7	120.8	123.1	123.3	122.6	120.6
Total evaporator inlet HFE7000 T (°C)	75.2	78.6	80.3	80.3	80.6	81.4	81.4
Total superheater outlet HFE7000 T (°C)	117.2	122.3	125.7	128.0	127.8	127.0	125.0
Condenser inlet water T (°C)	4.9	4.8	4.7	4.6	4.9	4.9	5.0
Condenser outlet water T (°C)	42.4	44.5	47.6	47.1	46.2	48.0	48.6
Expander inlet HFE7000 P_{t_in} (bars)	3.955	4.150	4.204	4.123	4.197	4.324	4.424
Expander outlet HFE7000 P_{t_out} (bars)	3.391	3.548	3.580	3.249	3.312	3.373	3.467
Expander pressure ratio, P_{t_in}/P_{t_out}	1.166	1.170	1.174	1.269	1.267	1.282	1.276
Total evaporator inlet HFE7000 P (bars)	5.027	5.39	5.584	5.837	6.014	6.228	6.391
Total superheater outlet HFE7000 P (bars)	4.836	5.098	5.184	5.26	5.404	5.653	5.862

[a] Calculated from the measured RPM of the expander.

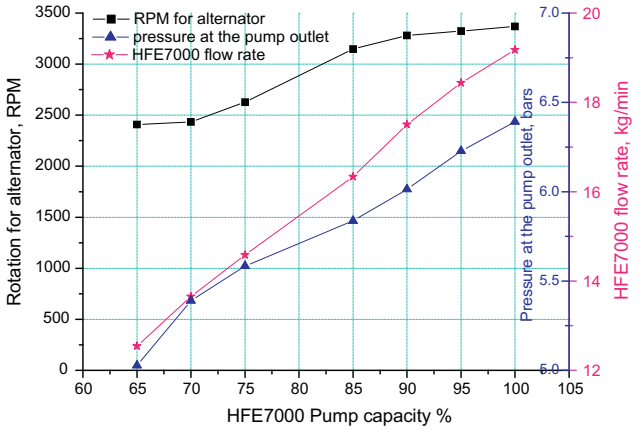

Fig. 6. Variations of the alternator RPM, organic working fluid flow rate and pressure at the pump outlet with the pump capacity (without alternator excitation).

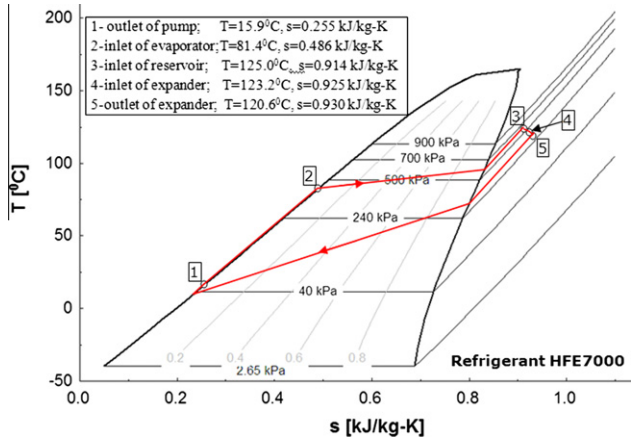

Fig. 7. HFE7000 working T–S chart without alternator excitation at the full pump capacity (from EES calculations [34]).

4.2. Biomass-fired CHP test results

To start a CHP test, the alternator has to be excited – the excitation of the alternator makes it possible to transform the mechanical energy of the expander (i.e. the shaft power of the expander) to electrical power. After the excitation, with the biomass boiler continuously operating (with a hot water temperature set point of 145 °C) and the organic working fluid pump operating at its full capacity, different electric loads could be connected to the output of the alternator and this led to not only different amounts of electricity generated but also different ORC temperatures and pressures as shown in Table 4 and Fig. 8, respectively. With a thermal input of 61.2 kW (calculated from the measured biomass pellet consumption rate – 12.73 kg/h and the low heating value of the biomass pellets – 4.8 kWh/kg) to the biomass boiler, the maximum electric power output of 860.7 W (12.08 V, 71.24 A) had been achieved with the electric load of 15 of 50 W-rated DC bulbs and 8 of 20 W-rated DC bulbs connected in parallel. The corresponding heat output with the cooling water flow of the condenser was found to be 47.26 kW_{th} as the cooling water was heated from 5.0 °C to 46.2 °C at a flow rate of 17 l/min. While the main temperatures and pressures measured under the conditions that had led to the maximum electric power output have already been shown in Fig. 3, the corresponding HFE7000 working T–S chart is shown in Fig. 9. Compared with the cases of 100% organic working fluid pump capacity in Table 3, Table 4 shows that the excited alternator RPM decreases sharply to nearly half of the RPM without the excitation, but the expander inlet pressure increases obviously and accordingly the expander pressure ratio increases, which results in the difference of T–S charts seen in Figs. 7 and 9. The other main ORC and system performance parameters with the case of the maximum power output of 860.7 W are also shown in Table 4.

The electricity generation efficiency of 1.41% is much smaller than that predicted by the thermodynamic modelling [7,8]. With an evaporator temperature of ca. 120 °C, the thermodynamic modelling predicted that the electrical efficiency of 8–9% [7,8]. There are two main factors responsible for the apparent difference in the electrical generation efficiency between the present experiments and the thermodynamic modelling: (1) the model assumed the expander efficiency of 85% [7,8], but the experimental results show that it is only 53.92%; (2) the model assumed that the alternator efficiency of 90% [7,8] but the experimental results show that it is only 50.94%.

The lack of commercially available micro-expanders is one of the main constraints for the development of micro-scale ORC-based CHP system. The use of the low cost and compact air motor-modified expander in the present experimental system proved to be feasible and successful [2] but the relatively low expander efficiency of ca. 54% is a concern. On the other hand, the connection between the expander and the alternator by a pulley and belt assembly is nowhere near ideal – the alternator efficiency of ca.

Table 4
Variations of parameters of ORC and power output under different electric loads with full refrigerant pump capacity.

Test cases: electric loads	1: 17 50 W bulbs	2: 18 50 W bulbs	3: 19 50 W bulbs	4: 15 50 W bulbs + 8 20 W bulbs	5: 16 50 W bulbs + 8 20 W bulbs	6: 19 50 W bulbs + 8 20W bulbs
Expander RPM	860	856	849	854	852	841
Alternator RPM[a]	1705	1697	1683	1693	1689	1667
HFE7000 flow rate $\dot{m}$ (kg/min)	18.43	18.43	18.43	18.43	18.43	18.43
Boiler inlet water T (°C)[b]	99.2	99.3	98.9	99.2	99.0	99.3
Boiler outlet water T (°C)	126.9	126.9	126.3	126.9	126.4	126.9
Expander inlet HFE7000 T (°C)	118.6	118.7	117.5	118.6	117.5	118.5
Expander outlet HFE7000 T (°C)	108.7	108.7	107.5	108.6	107.3	108.4
Total evaporator inlet HFE7000 T (°C)	84.8	85.1	84.9	85.3	85.3	85.2
Total superheater outlet HFE7000 T (°C)	120.2	120.2	118.9	120.2	118.9	120.0
Condenser inlet water T (°C)	5.0	5.0	5.0	5.0	5.0	5.0
Condenser outlet water T (°C)	45.8	45.9	45.6	46.2	45.5	45.8
Expander inlet HFE7000 P_{t_in} (bars)	6.649	6.66	6.669	6.674	6.699	6.724
Expander outlet HFE7000 P_{t_out} (bars)	3.22	3.219	3.206	3.236	3.218	3.21
Expander pressure ratio, P_{t_in}/P_{t_out}	2.065	2.069	2.080	2.063	2.080	2.095
Total evaporator inlet HFE7000 P (bars)	7.651	7.671	7.652	7.687	7.685	7.702
Total superheater outlet HFE7000 P (bars)	7.554	7.575	7.567	7.582	7.596	7.612
Electric power output, W	857.9	855.7	845.1	860.7	851.1	821.8
Expander shaft power output, kW	1.690	1.690	1.659	1.690	1.720	1.690
Expander efficiency %	53.40	52.88	52.94	53.92	55.45	52.38
Alternator efficiency %	50.77	50.64	50.94	50.94	49.47	48.64
ORC efficiency %	3.76	3.77	3.73	3.78	3.89	3.78
Boiler efficiency %	80.89	80.80	79.91	80.85	80.30	80.52
Electricity generation eff.%	1.40	1.40	1.38	1.41	1.39	1.34
Thermal efficiency %	76.63	76.63	76.05	77.28	76.06	76.56
Biomass CHP efficiency %	78.03	78.03	77.43	78.69	77.45	77.91

[a] Calculated from the measured RPM of the expander.
[b] Hot water flow rate – 28.27 l/m, biomass consumption rate – 12.74 kg/h, low heating value of the biomass fuel – 4.8 kWh/kg.

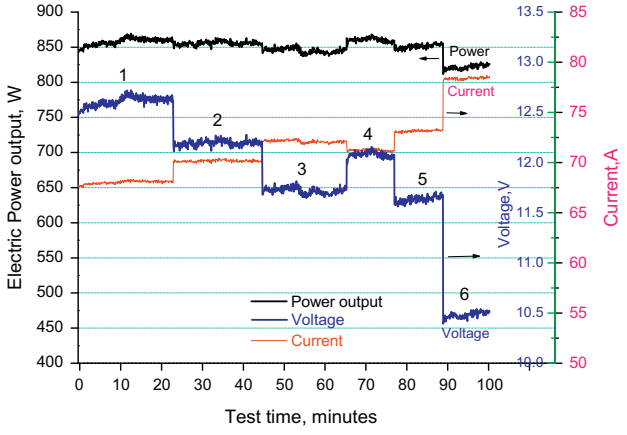

Fig. 8. Variations of power output, current and voltage under 8 different loads with the full refrigerant pump capacity (1:17 50 W-bulbs; 2:18 50 W-bulbs; 3: 19 50 W-bulbs; 4:15 50 W-bulbs + 8 20 W-bulbs; 5: 16 50 W-bulbs + 8 20 W-bulbs; 6: 19 50 W-bulbs + 8 20 W-bulbs).

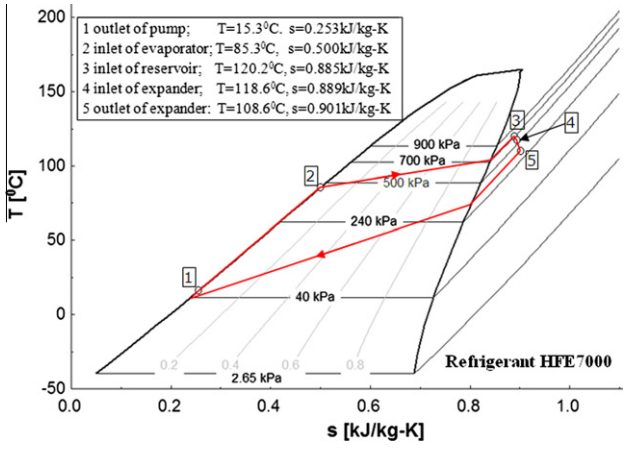

Fig. 9. HFE7000 working T–S chart with electricity generation at the full pump capacity (from EES calculations [34]).

51% was well expected. To improve the alternator efficiency, a different connection between the expander and alternator such as direct coupling may be considered in the future.

In addition, the current designs, particularly the heat exchanger, of the 50 kW_{th} biomass boiler used in the present study need to be modified in order to improve ORC efficiency. Thermodynamic modelling of the proposed micro-CHP system has shown that the ORC efficiency increases with the evaporator temperature [7,8]. The maximum hot water temperature achieved with the 50 kW_{th} biomass boiler is significantly lower than that was aimed for with the original design. The traditional single water-path type of heat exchanger which was used with the 50 kW_{th} boiler and many other domestic biomass boilers is not likely able to produce hot water with the temperature up to 180 °C and hence a new concept of heat exchanger for the biomass boiler such as a multi-water-path heat exchanger may be needed.

5. Conclusions

A micro-scale biomass-fired CHP with ORC has been constructed and tested with a 50 kW_{th} biomass boiler. The experimental setup and the latest experimental results are presented and discussed in this paper. The excitation of the alternator leads to a sharp decrease of the expander rotation speed and increases in the expander inlet pressure and expander pressure ratio. However, the excitation of the alternator is necessary for the transformation of the expander's mechanical energy to electricity. The experimental results show that the current biomass-fired ORC-based micro-

CHP system can generate electricity of 860.7 W and heat of 47.26 kW_{th}, corresponding to electricity generation efficiency 1.41% and CHP efficiency 78.69%. Under the conditions of achieving the above maximum power output, the efficiencies of the other main devices in the CHP system are the expander efficiency of 53.92%, the alternator efficiency of 50.94%, the boiler efficiency of 80.85% and the ORC efficiency of 3.78%.

The current biomass-fired CHP system has lower power output efficiency than that predicted by the thermodynamic modelling – the relatively low expander efficiency and low alternator efficiency of the current experimental system are the main factors that need to be addressed in the future. In addition, a new design of heat exchanger for the biomass boiler is also needed in order to generate hot water with the temperature up to 180 °C.

Acknowledgements

The authors wish to acknowledge the financial supports from the UK EPSRC (EP/E020062/1), Technology Strategy Board (TPQ3082A) and EPSRC Knowledge Transfer Secondment (RA4547) for their research work on the development of a biomass-fired ORC-based micro-CHP system. F-Chart Software (http://www.fchart.com/) is acknowledged for the provision of EES.

References

[1] Liu H, Qiu GQ, Shao YJ, Daminabo F, Riffat SB. Preliminary experimental investigations of a biomass-fired micro-scale CHP with organic Rankine cycle. Int J Low Carbon Technol 2010;5:81–7.
[2] Qiu GQ, Liu H, Riffat SB. Expander for micro-CHP systems with organic Rankine cycle. Appl Therm Eng 2011;31:3301–7.
[3] Bernotat K, Sandberg T. Biomass fired small-scale CHP in Sweden and the Baltic States: a case study on the potential of clustered dwellings. Biomass Bioenergy 2004;27:521–30.
[4] Dong LL, Liu H, Riffat SB. Development of small-scale and micro-scale biomass-fuelled CHP systems – a literature review. Appl Therm Eng 2009;29:2119–26.
[5] Bain RL, Overend RP, Craig KR. Biomass-fired power generation. Fuel Process Technol 1998;54:1–16.
[6] Hung TC, Shai TY, Wang SK. A review of organic Rankine cycles (ORCs) for the recovery of low-grade waste heat. Energy 1997;22:661–7.
[7] Castellana C, Liu H. Thermodynamic analysis of a biomass-fired micro-CHP with organic Rankine cycle. In: Eighth international conference on sustainable energy techologies: Aachen, Germany, 2009.
[8] Liu H, Shao YJ, Li JX. A biomass-fired micro-scale CHP system with organic Rankine cycle (ORC) – thermodynamic modelling studies. Biomass Bioenergy 2011;35:3985–94.
[9] Schmidt MC. Electric power research trends. New York: Nova science publishers, Inc.; 2007.
[10] Lemort V, Quoilin S, Cuevas C, Lebrun J. Testing and modeling a scroll expander integrated into an organic Rankine cycle. Appl Therm Eng 2009;29:3094–102.
[11] Quoilin S, Lemort V, Lebrun J. Experimental study and modeling of an organic Rankine cycle using scroll expander. Appl Energy 2010;87:1260–8.
[12] Peterson RB, Wang H, Herron T. Performance of small-scale regenerative Rankine power cycle employing a scroll expander. Proc Inst Mech Eng J Pow 2008;222:271–82.
[13] Wang H, Peterson RB, Herron T. Experimental performance of a compliant scroll expander for an organic Rankine cycle. Proc Inst Mech Eng J Pow 2009;223:863–72.
[14] Pei G, Li J, Li YZ, Wang DY, Ji J. Construction and dynamic test of a small-scale organic rankine cycle. Energy 2011;36:3215–23.
[15] Peng XY, Yang BC, Sun SY, Guo B, Xing ZW. Study of a rotary vane expander for the transcritical CO(2) cycle – Part I: experimental investigation. Hvac&R Res 2009;15:673–88.
[16] Yang B, Peng X, He Z, Guo B, Xing Z. Experimental investigation on the internal working process of a CO(2) rotary vane expander. Appl Therm Eng 2009;29:2289–96.
[17] Yang B, Peng X, Sun S, Guo B, Xing Z. A study of the vane dynamics in a rotary vane expander for the transcritical CO(2) refrigeration cycle. Proc Inst Mech Eng J Pow 2009;223:429–40.
[18] Jia XH, Zhang B, Yang BC, Peng XY. Study of a rotary vane expander for the transcritical CO(2) cycle – Part II: theoretical modeling. Hvac&R Res 2009;15:689–709.
[19] Liu GB, Zhao YY, Liu YX, Li LS. Simulation of the dynamic processes in a scroll expander–generator used for small-scale organic Rankine cycle system. Proc Inst Mech Eng J Pow 2011;225:141–9.
[20] Subiantoro A, Tiow OK. Introduction of the revolving vane expander. Hvac&R Res 2009;15:801–16.
[21] Subiantoro A, Ooi KT. Design analysis of the novel revolving vane expander in a transcritical carbon dioxide refrigeration system. Int J Refrig 2010;33:675–85.
[22] Li MX, Ma YT, Tian H. A rolling piston-type two-phase expander in the transcritical CO(2) cycle. Hvac&R Res 2009;15:729–41.
[23] Wang XD, Zhao L, Wang JL, Zhang WZ, Zhao XZ, Wu W. Performance evaluation of a low-temperature solar Rankine cycle system utilizing R245fa. Sol Energy 2010;84:353–64.
[24] Mago PJ, Chamra LM, Srinivasan K, Somayaji C. An examination of regenerative organic Rankine cycles using dry fluids. Appl Therm Eng 2008;28:998–1007.
[25] Chen HJ, Goswami DY, Stefanakos EK. A review of thermodynamic cycles and working fluids for the conversion of low-grade heat. Renew Sust Energy Rev 2010;14:3059–67.
[26] Tchanche BF, Papadakis G, Lambrinos G, Frangoudakis A. Fluid selection for a low-temperature solar organic Rankine cycle. Appl Therm Eng 2009;29:2468–76.
[27] Saleh B, Koglbauer G, Wendland M, Fischer J. Working fluids for low-temperature organic Rankine cycles. Energy 2007;32:1210–21.
[28] Drescher U, Bruggemann D. Fluid selection for the Organic Rankine Cycle (ORC) in biomass power and heat plants. Appl Therm Eng 2007;27:223–8.
[29] Guo T, Wang HX, Zhang SJ. Selection of working fluids for a novel low-temperature geothermally-powered ORC based cogeneration system. Energy Convers Manage 2011;52:2384–91.
[30] Guo T, Wang HX, Zhang SJ. Fluids and parameters optimization for a novel cogeneration system driven by low-temperature geothermal sources. Energy 2011;36:2639–49.
[31] Mago PJ, Chamra LM, Somayaji C. Performance analysis of different working fluids for use in organic Rankine cycles. Proc Inst Mech Eng J Pow 2007;221:255–64.
[32] Quoilin S, Declaye S, Tchanche BF, Lemort V. Thermo-economic optimization of waste heat recovery organic Rankine cycles. Appl Therm Eng 2011;31:2885–93.
[33] Liu H, Qiu GQ, Shao YJ, Riffat RB. Experimental investigation on the flue gas emissions of a domestic biomass boiler under normal and idle combustion conditions. Int J Low Carbon Technol 2010;5:88–95.
[34] Klein SA. Engineering equation solver (EES) for microsoft windows operating systems, professional versions, Madison USA, WI: F-chart software; 2011 <http://www.fchart.com>.